ISBN: 978-3-95450-218-9 ISSN: 2226-0374 doi:10.18429/JACoW-COOL2019-TUB02

PLASMA-CASCADE INSTABILITY

Vladimir N. Litvinenko [1,2 †], Gang Wang[2,1], Yichao Jing[2,1], Dmitry Kayran[2,1], Jun Ma[2], Irina Petrushina[1], Igor Pinayev[2] and Kai Shih[1]
[1] Department of Physics and Astronomy, Stony Brook University, Stony Brook, USA
[2] Collider-Accelerator Department, Brookhaven National Laboratory, Upton, USA

Abstract

In this paper we describe a new micro-bunching instability occurring in charged particle beams propagating along a straight trajectory. Based on the dynamics of this parametric instability we named it a Plasma-Cascade Instability. Such instability can strongly intensify longitudinal micro-bunching originating from the beam's shot noise, and even saturate it. On the other hand, such instability can drive novel high-power sources of broadband radiation. We discovered this phenomenon in a search of a broadband amplifier for Coherent electron Cooling [1,2], which does not require separating electron and hadron beams.

INTRODUCTION

High brightness intense charged particle beams play critical role in the exploration of modern science frontiers Such beams are central for high luminosity hadron colliders as well as for X-ray free-electron-lasers (FEL) with ultra-fast time structures reaching the femtosecond level. Dynamics of intense charged particle beams is driven by both external factors – such as focusing and accelerating fields - and self-induced (collective) effects.

While external factors are typically designed to preserve beam quality, the collective effects can result in an instability. Such instabilities can severely degrade beam quality by spoiling its emittance(s) – increasing beam's momentum spread or creating density modulation or even filamentation in the beam. On the other hand, such instabilities can be deliberately built-in to attain specific results [1-6]. The Plasma-Cascade micro-bunching Instability (PCI) occurs in a beam propagating along a straight line. By its nature, the PCI is a parametric instability driven by variation of the electron beam density and corresponding change of the plasma oscillation frequency [5]. Conventional micro-bunching instability in beams travelling along a curved trajectory (for example, in a magnetic chicane or in an arc of an accelerator) is a well-known. But none of them includes PCI –a micro-bunching longitudinal instability driven by modulations of the transverse beam size.

PLASMA-CASCADE INSTABILITY

We start from a qualitative description of the PCI, which will be followed by rigorous theory, 3D simulations and experimental observation of this phenomena. Figure 1 depicts periodic focusing structure where the charged particle beam undergoes periodic variations of its transverse size. It is known small electron density perturbations $\tilde{n}(\vec{r}), |\tilde{n}| << n_o$ in a cold, infinite and homogeneous plasma will result in oscillations with plasma frequency, ω_p [7]:

$$\frac{d^2\tilde{n}}{dt^2} + \omega_p^2 \tilde{n} = 0;\ \omega_p = c\sqrt{4\pi n_o r_c}, \qquad (1)$$

where n_o is the particles density (in our case, in the beam's co-moving frame), c is the speed of the light and $r_c = e^2/mc^2$ is classical radius of the particles.

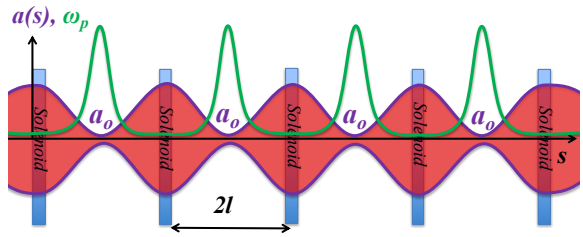

Figure 1: A sketch of four focusing solenoids cells with periodic modulations of beam envelope, *a(s),* and the plasma frequency, ω_p. Beam envelope has waists, a_o, in the middle of each cell where plasma frequency peaks. Both vertical and horizontal scale are optimized for illustration of the process.

For the beam propagating with velocity v_o in the periodic lattice with period *2l*, shown in Fig. 1, it would lead to a periodic modulation of the density $n_o \sim 1/a^2$ and the plasma frequency $\omega_p \sim 1/a$ with a period of $T = 2l/\gamma_o v_o$, where we took into account the relativistic time dilation in the co-moving frame by the beam's relativistic factor $\gamma_o = \left(1-\beta_o^2\right)^{-1/2}, \beta_o = v_o/c$. It is well known in classical oscillator theory [8] that rigidity modulation close to a half of oscillation period would result in exponential growth of oscillation amplitude: the phenomena known as parametric resonance. The extreme case of δ-function-like modulation is also well known: periodic focusing lenses with focal length is shorter than a quarter of the separating distances a ray instability in system. Hence the modulation of the transverse size could, in principle, results in unstable, e.g. growing longitudinal oscillation density. Such instability can also be a result of aperiodic frequency modulation: it is well known in accelerator physics that a solution of *s*-dependent Hill's equation, *x"+K(s)x=0*,can lead to unstable oscillations in focusing system with *K(s)>0.*

Analytical Studies

To switch from qualitative to qualitative description of PCI we need to identify a problem which is analytically tractable. In mathematical terms, we need to separate transverse and longitudinal degrees of freedom. As shown in [5,6] desirable separation is possible for long bunch, σ_s

† vladimir.litvinenko@stonybrook.edu

ISBN: 978-3-95450-218-9 ISSN: 2226-0374 doi:10.18429/JACoW-COOL2019-TUB02

$(\gamma_o\sigma_s >> a)$ with transverse Kapchinsky- Vladimirsky (KV) distribution [9]:

$$f_\perp(x,x',y,y') = N\cdot\delta\left(\frac{x^2+y^2}{a^2}+\frac{(ax'-a'x)^2+(ay'-a'y)^2}{\varepsilon^2}-2\right); \quad (2)$$

where ε is the envelope emittance. The KV beam has uniform density is uniform within the beam radius, defined by the envelope $r \le a(s)$, and zero density outsize it. Uniform particle's density results in linear defocusing electric field, which in combination with linear transverse focusing, preserves the KV distribution (2) with self-consistent beam envelope defined by a nonlinear equation [10]:

$$\frac{d^2a}{ds^2}+K(s)a-\frac{2}{\beta_o^{\,3}\gamma_o^{\,3}}\frac{I_o}{I_A}\frac{1}{a}-\frac{\varepsilon^2}{a^3}=0;\ K(s)=\left(\frac{eB_{sol}(s)}{2p_oc}\right)^2 \quad (3)$$

where I_o is the beam current, $p_o=\gamma_o\beta_o mc$ is particles momentum, and K is external focusing provided by solenoids and $I_A = mc^3/e \approx 17\ kA$ is Alfven current. With few exceptions [5,6] this has to be solved numerically to define the density (in the co-moving frame):

$$f_\perp = n_o(t) = \frac{I_o}{e\beta_o\gamma_o c}\frac{1}{\pi a^2(\gamma_o\beta_o ct)}. \quad (4)$$

Let's consider the distribution function in the co-moving frame as a weak perturbation $\tilde{f}$, $|\tilde{f}| << f_o$:

$$f = f_\perp\cdot f_\parallel(z,\mathrm{v},t);\ f_\parallel(z,\mathrm{v},t) = f_o(\mathrm{v})+\tilde{f}(z,\mathrm{v},t), \quad (5)$$

where v is z-component of velocity. Evolution of $\tilde{f}$ described by a linearized set of Vlasov- Poisson equations [11], $\tilde{n}(z,t) = n_o(t)\cdot\int_{-\infty}^{\infty}\tilde{f}\,d\mathrm{v}$:

$$\frac{\partial}{\partial t}\tilde{f}+\mathrm{v}\frac{\partial\tilde{f}}{\partial t}+\frac{eE_z}{m}\cdot\frac{\partial f_o}{\partial \mathrm{v}}=0;\ \frac{\partial E_z}{\partial z}=4\pi e\tilde{n}. \quad (6)$$

To exclude transverse components of the electric field in (6), e.g. for complete separation of longitudinal and transverse degrees of freedom, we added additional requirements for the longitudinal modulation: it has to at wavelength much shorter than the beam radius $\lambda_m << a$ [5]. Following technique developed in [12]: assuming κ-1 longitudinal velocity distribution $f_o(\mathrm{v}) = \sigma_\mathrm{v}/\pi(\sigma_\mathrm{v}^{\,2}+\mathrm{v}^2)$ and applying Fourier transformation $f_k = \int f\exp(-ikz)dz$ reduces eq. (7) to an oscillator equation:

$$\frac{d^2\tilde{n}_k}{dt^2}+\omega_p^2(t)\tilde{n}_k=0;\ \tilde{n}_k = \exp(|k\sigma_\mathrm{v}t|)\int_{-\infty}^{\infty}\tilde{f}_k(\mathrm{v})d\mathrm{v}; \quad (7)$$

for density perturbation corrected by Landau damping $\exp(|k\sigma_\mathrm{v}t|)$ term. Solution of eq. (7) can be expressed using symplectic ($det\,\mathbf{M}$=1) matrix: $X(t) = \mathbf{M}(0|t)\cdot X_o$:

$$\mathbf{M}(0|t) = \exp\left(\int_0^t\mathbf{D}(\tau)\,d\tau\right);\ \mathbf{D}(t)=\begin{bmatrix}0 & 1\\ -\omega_p^2(t) & 0\end{bmatrix}, \quad (8)$$

with either stable or growing solutions determined by the matrix's eigen values $\lambda_{1,2}:\det[\mathbf{M}-\lambda_{1,2}\cdot\mathbf{1}]=0;\ \lambda_1\lambda_2=\det\mathbf{M}=1\cdot$

Periodic system comprised of n bilaterally-symmetric cells, such as shown in Fig. 1, allows a well-defined parametric study of the PCI growth rates:

$$\mathbf{M}(0|nT)=\mathbf{M}_c^{\,n};\ \mathbf{M}_c\equiv\mathbf{M}(0|T)=\begin{bmatrix}m_{11} & m_{12}\\ m_{21} & m_{11}\end{bmatrix}; \quad (9)$$

$$\lambda_1 = m_{11}-\sqrt{m_{11}^{\,2}-1};\ \lambda_2=\lambda_1^{-1};$$

$|m_{11}|>1$ and signal evolution as:

$$X(mT)=\begin{bmatrix}\tilde{n}(mT)\\ \dot{\tilde{n}}(mT)\end{bmatrix}_o=\begin{bmatrix}g_+\\ g_-/b\end{bmatrix}\tilde{n}_o+\begin{bmatrix}\mathrm{b}\cdot g_-\\ g_+\end{bmatrix}\dot{\tilde{n}}_o; \quad (10)$$

$$g_+=\frac{\lambda_1^m+\lambda_1^{-m}}{2};\ g_-\frac{\lambda_1^m-\lambda_1^{-m}}{2};\ \mathrm{b}=\frac{-m_{12}}{\sqrt{m_{11}^{\,2}-1}}.$$

Additional utility of periodic (cell) structure is dimensionless form of equations (3) and (7):

$$\frac{d^2\hat{a}}{d\hat{s}^2}-k_{sc}^{\,2}\hat{a}^{-1}-k_\beta^{\,2}\hat{a}^{-3}=0;$$
$$\frac{d^2}{d\hat{s}^2}\tilde{n}_k+2\frac{k_{sc}^2}{\hat{a}(\hat{s})^2}\cdot\tilde{n}_k=0;\ \hat{a}=\frac{a}{a_o};\ \hat{s}=\frac{s}{l}, \quad (11)$$

with well-defined dimensionless variables $\hat{a}\ge 1;\ \hat{s}\in\{-1,1\}$ and the system dynamics fully defined by two dimensionless parameters

$$k_{sc}=\sqrt{\frac{2}{\beta_o^{\,3}\gamma_o^{\,3}}\frac{I_o}{I_A}\frac{l^2}{a_o^{\,2}}};\ k_\beta=\frac{\varepsilon l}{a_o^{\,2}},$$

representing space charge and emittance effects. Figure 2 shows the growth rate per cell in such system evaluated by a semi-analytical code in Mathematica using 4-th order symplectic integrators [12] with canonical Hamiltonians:

$$\hat{h}=\frac{\hat{a'}^2}{2}-k_{sc}^2\ln\hat{a}+\frac{k_\beta^2}{2\hat{a}^2}=\frac{k_\beta^2}{2}=inv;\ \hat{h}(s)=\frac{\tilde{n}_k'^2}{2}+\frac{k_\beta^2}{\hat{a}^2(s)}\tilde{n}_k^{\,2}.$$

Growth rate with λ=4 can be reached with modest parameters of k_{sc}=3 and $k_\beta=10$. A "ridge" with maximum growth rates approximately following the line $k_\beta = 3\cdot(k_{sc}-1.2)$ with growth rate approximated by $\lambda\propto 1.25k_{sc}\approx 1.5+0.413\,k_\beta$. While λ does not contain any dependence on the wavelength of modulation ($k=2\pi/\lambda_m$), or corresponding frequency of modulation in the lab-frame ($\omega_m=\gamma_o\mathrm{v}_o k$), the PCI growth is inhibited both at high and low frequencies. At high frequencies the growth is limited by Landau damping (7) to

$$k_{\max}=\frac{\ln\lambda}{T\sigma_\mathrm{v}};\ \omega_{\max}=\frac{\mathrm{v}_o}{2l}\cdot\frac{\gamma_o^{\,3}}{\sigma_\gamma}\ln\lambda,$$

ISBN: 978-3-95450-218-9 ISSN: 2226-0374 doi:10.18429/JACoW-COOL2019-TUB02

where is σ_γ / γ_o is the relative energy spread in the beam, related to the velocity spread in the co-moving frame as: $\sigma_\gamma / \gamma_o = \sigma_v / c$. Analytical studies of modulation at low frequencies are rather elaborate (see [5,6]) and here we provide an approximate scaling at low frequencies of space charge coefficient $k_{sc} \to k_{sc} \cdot \left(k\langle a(s)\rangle\right), k\langle a(s)\rangle < 1$.

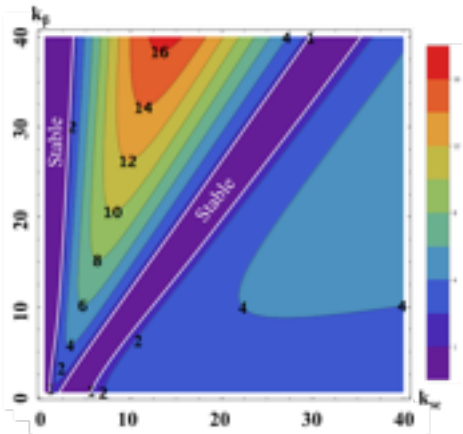

Figure 2: Contour plots of $\lambda = \max\left(\left|\mathrm{Re}\,\lambda_1\right|, \left|\mathrm{Re}\,\lambda_2\right|\right)$, the absolute value of maximum growth rate per cell. Purple area highlighted by white lines indicates areas of stable oscillation $\left|\lambda_{1,2}\right| = 1$. Oscillations, e.g. density modulations, grow exponentially outside these areas. Instability vanished at low cut-off frequency, when the "working point" k^*_{sc}, k_β reaches stable region.

Table 1: Parameters for PCI Simulations and Tests

Name	Experiment	Case 1	Case 2
PCA	LEBT	4 sec.	4 sec.
γ	3.443	28.5	275
E, MeV	1.76	14.56	140.5
l, m	Var, 1.5 - 3	1	10
a_0, *mm*	Min 0.3	0.2	0.1
I_0, A	1.75	100	250
ε_{norm}, *m*	$1\ 10^{-6}$	$8\ 10^{-6}$	$4\ 10^{-4}$
k_{sc}	Varies	3.56	3.76
k_β	Varies	7.02	14.55
λ_1, per cell	N/A	-4.06	-5.10
Energy spread	$1\ 10^{-4}$	$1\ 10^{-4}$	$1\ 10^{-4}$
f, THz	0.4	25	1,000

Numerical Studies

While both qualitative and semi-analytical studies reveal the nature of the PCI, modern particle-in-cell codes allow 3D investigations of PCI without any predetermined assumption. We used code SPACE [13-15] for accurate simulation of PCI in electron beam with constant beam energy propagating along the straight section with focusing solenoids. Two samples of such simulations. with parameters listed in Table 1, are shown in Fig. 3. In both cases density modulation grew by about 100-fold in a 4-cell system. Solenoid strengths were selected to provide the designed value of the beam envelope, a_o, at the waists located in the middle of the cells. Amplitude of density modulation, $\tilde{n}_k$, was then tracked as a function of the propagation distance. Figure 3 clearly demonstrate the nature of this instability: in a quarter of a plasma oscillation, the density modulation is transferred into the velocity modulation (at locations of the density minima). In return, in the next quarter of plasma oscillation, the velocity generates larger density modulation (but with an opposite sign). This cascade-type process of plasma oscillation is the origin of the name for this instability—PCI. Our 3D simulations also confirmed analytical expectation that PCI is a broad-band instability. They also clearly indicate, that as predicted by analytical studies, the PCI is diminishing both at low and high frequencies. In contrast to 1D analytical description, the 3D SPACE provides information about spatial distribution of the evolving density modulation. Figure 4 illustrates these additional features, including bending of the modulation wave-fronts.

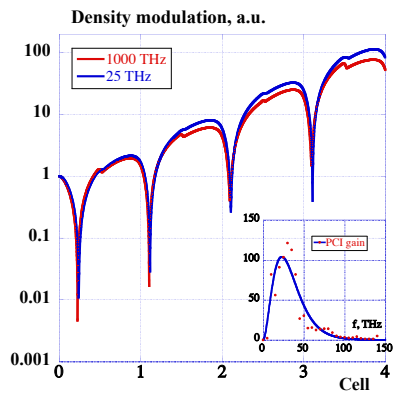

Figure 3: Evolution of density modulation amplitude in 4-cell PCI periodic lattice with parameters shown in Table 1: Blue line, *Case 1*, gain = 114 (b) Red line, *Case 2*, gain=75. The PCI gain spectrum for Case 1 in shown in a clip in the bottom-right corner: All simulations were performed by 3D code SPACE.

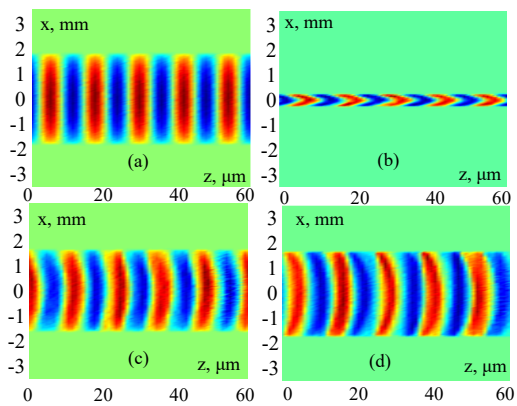

Figure 4: Evolution of the 3D profile of the e-beam density modulation at 25 THz (Case 1). Only normalised AC portion of the density is shown: red color corresponds to

ISBN: 978-3-95450-218-9 ISSN: 2226-0374 doi:10.18429/JACoW-COOL2019-TUB02

increased density and blue to reduced beam density. (a) – at the system entrance; (b) in the middle of the 2nd cell (beam waist); after the 3rd cell and (d) after 4-cell system.

Experimental Demonstration

Two room temperature RF 500 MHz cavities were used to correct the RF curvature and reducing energy spread in the bunch to 0.01% level. Six solenoids in the low energy beam transport (LEBT) were used for strong-focusing aperiodic lattice providing beam envelope shown in Fig. 5. To observed density modulation expected from very strong PCI we transformed our SRF linac and dipole beamline system in time-resolving system with sub-psec time resolution. We operated the linac at zero crossing with low accelerating voltage, V ~100-200 kV, to correlate particle's energy with the arriving time $E = E_o + eV\sin\omega_L t$. The 45º dipole and the profile monitor 4 served energy spectrometer: the measured energy distribution was a carbon copy for time profile of the bunch. We found that the best data quality was obtained at 100 kV setting and Fig. 6 shows few selected density profiles measured by our system as well as their spectra. We observed very large, up to ±50%, density modulation that can be seen both captured images or density profiles in Fig.6 (a) and (c). Fig. 6 (b) shows measured bunch spectra, which compare very well with simulation: a broadband PCI gain breaking at ~ 0.4 THz. We also calculated correlation length of the density modulation to be ~ 1-2psec, which is in good agreement with the spectral bandwidth $\Delta f/f \sim 1$.

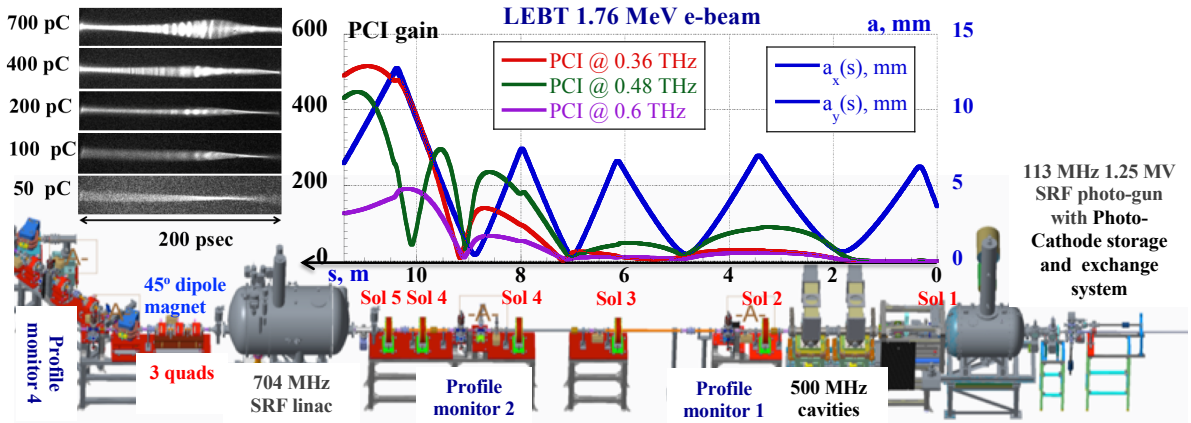

Figure 5: Layout of the CeC accelerator with the SRF electron gun, two bunching RF cavities, the LEBT line equipped with six solenoids and two profile monitors, the 13.1 MeV SRF linac and a 45º bending magnet beam line with beam profile monitor. The top graph shows simulated evolutions in the LEBT of the beam envelope (*a(s)*, blue line) and PCI gains at frequencies of 0.36 THz (red line), 0.48 THz (violet), and 0.6 THz (green). Simulations were done with for 1.75 MeV (γ=3.443), 0.7 nC, 0.4 nsec electron bunch with 1 μm slice normalized emittance and 0.01% slice RMS energy spread. Clip in the left-top corner shows time-resolve bunch profiles measured by the system for various charge in 400 psec electron bunches.

Because of the random nature of amplified shot noise, each bunch had its individual time structure and it was critical to measure structure of individual bunches in a single shot.

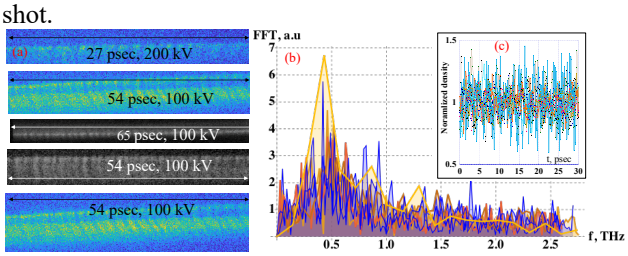

Figure 6: Measured (a) time profiles of the 1.75 MeV electron bunched bunch emerging from LEBT (charge per bunch from 0.45 nC to 0.7 nC). (b) Shows seven overlapping spectra of the bunch density modulation and PCI spectrum simulated by SPACE (slightly elevated yellow line). (c) Clip show 30-psec cut-off of seven measured density modulation.

In conclusion, we would like to announce discovery of novel microbunching instability occurring in charged particle beams propagating along a straight trajectory—Plasma-Cascade Instability. PCI can be both a menace and a blessing—it can strongly intensify longitudinal microbunching originating from the beam's shot noise, and even saturate it. For example, PCI can serve as a broadband amplifier in the CeC scheme [5,6] or used for boosting power of THz and PHz radiation.

Authors would like to thank all our colleagues from BNL contributed to the CeC project: Toby Miller high precision beam profile monitor diagnostics, Thomas. Hayes, Geetha Narayan and Freddy Severino for their help with using CeC SRF linac for time resolved studies, Dr. Peter Thieberger for pointing on important 3D aspects of the problem, and Dr. Thomas Roser for unrelenting support of this research. First author also would like to thank Prof. Pietro Musumeci (UCLA), who mentioned during our discussion about energy conservation in longitudinal plasma oscillations, that modulation of the transverse beam size

ISBN: 978-3-95450-218-9 ISSN: 2226-0374 doi:10.18429/JACoW-COOL2019-TUB02

can violate this perception. His notion was one of the initial signals that modulation of the transverse beam size can cause an instability. This research was supported by and NSF grant PHY-1415252, DOE NP office grant DE- FOA-0000632, and by Brookhaven Science Associates, LLC under Contract No. DEAC0298CH10886 with the U.S. Department of Energy.

REFERENCES

[1] V.N. Litvinenko, Y.S. Derbenev, "Coherent Electron Cooling", *Phys. Rev. Lett.* **102**, 15801, 2009.
[2] D. Ratner, "Microbunched Electron Cooling for High-Energy Hadron Beams", *Phys . Rev. Lett*. **111** 084802, 2013.
[3] V.N. Litvinenko, Y.S. Derbenev, in *Proc. of 29th International Free Electron Laser Conference* (FEL'07), Novosibirsk, Russia, 2007, p. 268.
[4] V.N. Litvinenko, "Advances in Coherent Electron Cooling", In *Proc. of COOL 2013 workshop*, June 2013, Mürren, Switzerland, p. 175, ISBN 978-3-95450-140-3.
[5] V.N. Litvinenko, G. Wang, D. Kayran, Y. Jing, J. Ma, I. Pinayev, "Plasma-Cascade micro-bunching Amplifier and Coherent electron Cooling of a Hadron Beams", arXiv:1802.08677, February 2018.
[6] V.N. Litvinenko, G. Wang, Y. Jing, D. Kayran, J. Ma, I. Petrushina, I. Pinayev, K. Shih, Plasma-Cascade Instability- theory, simulations and experiment, 2019, arXiv:1902.10846.
[7] D.R. Nicholson, Introduction in Plasma Theory, John Wiley & Sons, 1983.
[8] L.D. Landau, E.M. Lifshitz, Classical Mechanics, Elsevier Science, 1976, ISBN-10 050628960.
[9] I.M. Kapchinsky and V.V. Vladimirsky, in *Proc. of Int. Conf. on High-Energy Accelerators and Instrumentation,* CERN, 1959, p. 274.
[10] M. Reiser, Theory and design of charged particle beams, John Wiley & Sons, 2008.
[11] A. A. Vlasov, "On Vibration Properties of Electron Gas", *J. Exp. Theor. Phys.* (in Russian). 8 (3) 1938, 291.
[12] G.Wang, M.Blaskiewicz, *Phys Rev E*, volume 78, 026413, 2008.
[12] E. Forest, "Forth-order symplectic integrator", SLAG-PUB-5071, LBL-27662, August 1989.
[13] X. Wang, R. Samulyak, J. Jiao, K. Yu, "Adaptive Particle-in-Cloud method for optimal solutions to Vlasov-Poisson equation", *J. Comput. Phys.,* 316, pp. 682-699, 2016.
[14] K. Yu and V. Samulyak, "SPACE Code for Beam-Plasma Interaction", in *Proc. 6th Int. Particle Accelerator Conf. (IPAC'15)*, Richmond, VA, USA, May 2015, pp. 728-730. doi:10.18429/JACoW-IPAC2015-MOPMN012
[15] V.N. Litvinenko, Z. Altinbas, R. Anderson, S. Belomestnykh, C. Boulware *et al*., "Commissioning of FEL-based Coherent electron Cooling system", In *Proc. of 38th Int. Free Electron Laser Conf.* (FEL'17), Santa Fe, NM, USA, August 20-25, 2017, p. 132.